Elastohydrodynamic film thickness and temperature measurements in dynamically loaded concentrated contacts : eccentric cam-flat follower

Paper XX(ii)

Elastohydrodynamic film thickness and temperature measurements in dynamically loaded concentrated contacts: eccentric cam–flat follower

H. van Leeuwen, H. Meijer and M. Schouten

This paper describes some results of local film thickness and temperature measurements in an eccentric cam-flat follower contact by means of miniature vapour deposited thin layer transducers. Complex transducer patterns can be realized by employing photolithography, allowing local measurements in axial direction. A full film will develop at relatively low speeds. At high speeds chemical reaction layer formation starts. Film thickness and temperature at both sides of the contact differed appreciably, thus invalidating the assumption of line contact. Under high loads and misalignment a constriction in the film thickness, typically for EHD contacts, appears at the heavy load side. Only after supporting the follower on a self-aligning elastic hinge, a line contact condition could be attained. Temperature variations of the follower surface were found to be moderate. The transducers worked well and have a satisfying life expectancy.

1 INTRODUCTION

Research in full film lubrication of concentrated contacts under steady state conditions has a long history. Many examples can be found in the literature, e.g. Martin (1), Grubin (2), Blok (3), Dowson and Higginson (4), Herrebrugh (5), Hamrock and Dowson (6), and Ertel (7). This resulted in the well established approximative formulae for minimum and central film thickness of line and elliptical contacts, which proved to be a valuable part of the designer's toolkit. In all these cases constant load, entrainment velocity and curvature are assumed. These presumptions are very often satisfied in full film lubricated concentrated contacts. Hence, a quasi-stationary analysis will often yield good results. A graphical survey of these solutions is presented in Fig.1.

However, sometimes concentrated contacts experience variations in load, tangential surface velocity, or curvature, too large to admit a quasi-steady approach. In addition to entrainment, squeeze action helps in fluid film formation. After many investigators of non-steady state engine bearings, concentrated contacts having both entrainment and squeeze action will be designated "dynamically loaded". This adjective is preferable to the connotation "instationary", which has a different meaning in fluid mechanics.

The problem of normal approach of deforming bodies, without entrainment, has received attention from some authors, the first one being Christensen (8). Herrebrugh (9) presents an elegant method for the isoviscous squeeze film between two elastic cylinders. Vichard (10) gives a comprehensive analysis of the case of combined entrainment and squeeze action, using a Grubin/Ertel type of approach. Although this paper is published 15 years ago, it is the most authoritative in this field. Holland's (11) method, even though it has been corrected in details by Haiqing et al (12), suffers from the elementary error that, under conditions of EHD lubrication, Reynold's equation is no longer linear in the pressure, hence making the superposition principle invalid. Therefore, it will lead to erroneous results. Oh (13) solves the moderately loaded case, using the promising complementarity method, but needs unrealistic high load frequencies to obtain any marked squeeze effect.

A quasi-steady analysis will often suffice, but will definitely fail when the entrainment velocity momentarily equals zero. Piston ring-cylinder liner and (many) cam-follower contacts show this behaviour. Therefore, they are fine examples of dynamically loaded concentrated contacts.

It can be expected that computer simulations of dynamically loaded concentrated contacts will soon be able to predict the behaviour more accurately. Thus, there is a need for an independent verification by detailed experimental results. Theoretical models yield film thickness, pressure, and temperature distributions in space as a function of time. Experiments result in distributions in time as a function of position in space. Experiment and theory can only be compared if the data are converted into the same way of representation. Therefore, many experiments with a high resolution are needed. The film thickness plays a critical role from a designer's point of view. However, the literature is rather scarce on this point, as can be concluded from the following brief survey.

Pure squeeze flows in highly loaded point contacts are studied by Paul and Cameron (14), (15), and by Safa and Gohar (16). The former ones study local film thickness, using optical interferometry, and deduce viscosity behaviour from this, while the latter ones obtain pressure data as a function of position and

time by means of small vapour deposited transducers.

Combined entrainment and squeeze effects are found in piston ring-cylinder liner and cam-follower contacts. It is surprising to learn that most experiments on piston rings are performed on working engines, or motored test rigs made from stripped down engines, whilst the bulk of reports on cam mechanisms describe experiments with specially designed test rigs.

Examples of piston ring experiments can be found in (17)-(23). The rings in these references have a diameter of the order of 100 mm, except the crosshead diesel engine (23), which has a cylinder bore of 570 mm. The ring width is of the order of 2.5 to 10 mm. The mode of the lubrication is often intermediate elastohydrodynamic, which means that loads are moderate (24).

Pressure measurements are carried out in (17), (18) and (23), using piezoelectric transducers of 0.25 or 0.20 mm. effective diameter. In (19) and (20) the film thickness is monitored by electrical oil film resistance. Other techniques employed in film thickness experiments are capacitance measurements (17), (18), (19), and (21), or inductance measurements (22), (23), using a proximity probe. Transducer dimensions are 0.25-0.5 mm in the former, 2-4 mm in the latter case.

In (10) and (25)-(34) cam-follower experiments are described. In all test rigs the cam radius was of the order of 50 mm, while the cam width was of the order of 10 to 20 mm. Film thickness is estimated from global capacitance in (10), (25), (30) and (31), and from overall contact resistance in (26). Local film thickness measurements, employing the 0.25 mm dia. gauge described in (18), are reported in (29). The loads are rather low. This paper also shows pressure measurements obtained with a 0.25 mm effective dia. piezoelectric transducer. Local pressures and temperatures can also be obtained using miniature thin film transducers, see (27), (28), (32) and (33). These transducers have a minimum width of 10 μm. To find local cam surface temperatures, an infrared scanning system was employed in (34), with a spot size of 0.45 mm.

Steinführer (35), and Coy and Dyson (36) describe cam-follower test rigs, designed to simulate the peculiar vanishment of entrainment effects of many cam mechanisms. In (35) the average film thickness is found by an indirect measurement of capacitance, while (36) describes profile measurements of cam and follower, leading to the conclusion that hydrodynamic effects are important, even when the estimated film thicknesses are much smaller than the surface roughness.

Piston ring experiments are troublesome because of the many degrees of freedom of the ring, and the number of transducers which can be mounted, thus limiting the number of transducer positions. The mode of lubrication is intermediate or medium elastohydrodynamic.

A cam-flat follower geometry allows the transducer to be positioned at any wanted location (see section 3), thus permitting many measurements. The mode of lubrication is medium till full elastohydrodynamic, or mixed film. The literature provides some local film thickness and pressure distributions in the piston ring case, and some global film thickness and local pressure and temperature measurements in the cam-follower case. Much more experimental data are needed, in particular on film thickness distributions. Thus it was thought important to carry out local film thickness and temperature measurements in a cam-flat follower contact. This paper describes initial results obtained with an eccentric cam.

1.1 Notation

b	Hertzian semi-contact width	m
c	spring stiffness in cam-follower test rig	N/m
C	capacitance	F
E_r	reduced modulus of elasticity	N/m^2
F_*	load	N
F	reference load	N
g_E	elasticity number	-
g_F	load number	-
g_u	speed number	-
g_s	squeeze number	-
g_v	pressure-viscosity number	-
g_w	entrainment number	-
h_{min}	minimum film thickness	m
h	dimensionless minimum film thickness $h=h(g_E,g_v)$	-
H	dimensionless minimum film thickness $H=H(g_u,g_F)$	-
l	contact length	m
m	reciprocating mass in cam-follower test rig	kg
p	fluid film pressure	N/m^2
R	resistance	Ohm
R_r	reduced contact radius	m
t	time	s
T	temperature	C
u	rolling speed	m/s
α	pressure viscosity coefficient	m^2/N
η	dynamic viscosity	Ns/m
θ	dimensionless time, $\theta=\omega t$; at maximum lift $\theta=0$	-
Λ	relative film thickness, $\Lambda=h_{min}/\sigma$	-
σ_{Hz}	maximum Hertzian pressure	N/m^2
σ	composite RMS surface roughness value	m
ω	rotational speed	s^{-1}

2 FULL FILM LUBRICATION IN CAM MECHANISMS

Due to surface roughness, many concentrated contacts operate in the mixed film lubrication region. A fluid film in a concentrated contact is an extremely stiff element, which can, after some running in, result in full film lubrication conditions (36), even at elevated temperatures (37). Anyway, as long as the contacting asperities share only a small portion of the total load, full film considerations can still provide reliable design directives.

As the experiments to be carried out are needed to verify full film theoretical results, precautions have to be made to assure that the theoretical assumptions are met as close as possible. The most important influential variable is the oil viscosity. Hence a high viscosity oil was selected, and experiments were carried out at room temperature. This will at the same time prevent additive effects, if

formulated oils are used. The speed should be sufficiently high to ensure seperation of the contact surfaces. Very high speeds have to be avoided to prevent high film temperatures, hence viscosity thinning and surface film formation, see Section 4.2.

3 TEST RIG

The test apparatus used in this study has been described elsewhere (27),(28), so only brief details will be given here. A horizontally mounted camshaft 1 (see Fig.2) lifts a piston-like follower body 2 in a horizontal plane. This follower is supported by a double hydrostatic bearing 3. A load cell 4 measures the normal load in the contact. Follower, support bearing and load cell are mounted in one unit, which can traverse across the cam in a vertical plane by means of a precision linear bearing, connecting it to the steady support. This motion is indicated in Fig.3 by a vertical arrow. By doing so, it is possible to bring every point on the follower into contact with the cam. Thus it is possible to investigate the complete cam cycle with one single transducer; the transducer is fixed on the follower. During normal operation, each point on the follower contacts two points on the cam, see Fig.3, if it is located in the sliding area. This is a specific feature of cam mechanisms. Hence, two times per cycle a transducer will detect a signal. In Fig.3 corresponding cam and follower positions are marked. A transducer located at position 1 on the follower will produce a signal as long as the cam base circle is in contact. At position 2 it will yield a time dependent signal when points 2 and 3 on the cam contact the follower, and so on.

The camshaft is supported in precision single row angular contact ball bearings. As the cam is not crowned, alignment with the follower is essential. Precautions were taken to realize a very good alignment. A check of the footprint with Prussian blue indicated a misalignment of less than 2 μm over the contact length.

Just as in many modern automotive engines, it was decided to employ follower plates, which can be changed much easier than a complete follower. Because of their compact size and simple shape they are easy to manufacture and fit in most evaporation jars.

To assure full film lubrication, a copious supply of oil is necessary. Former experiences with a pin and disc machine learn that jet lubrication will be convenient. An extreme pressure gear oil was chosen because of its high dynamic viscosity and high pressure-viscosity coefficient.

A quasi-steady calculation of the cam-follower contact learns that film thicknesses of the order of 1 μm and even smaller can be expected. This necessitates a filter which will arrest all particles larger than 3/4 of the minimum film thickness. Absolute submicron filters do not permit a sufficiently large fluid flow in main stream applications, so it was decided to put it in a bypass, see Fig.4. The main stream contains a large hydraulic filter 4. From there the stream is divided over three parallel flows, i.e. the double hydrostatic bearing 2, the absolute filter 3 and the jet 1. Eventually all fluid will arrive at a large sump with a capacity of about 50 l. Oil quality can be checked by means of sampler 5.

Some numerical data of the test rig are given in Table I.

Maximum load		2000 N
Speed		
	minimum	$2.45\ s^{-1}$
	maximum	$34.5\ s^{-1}$
	nonuniformity	1 %
Cam	width	$17.5 * 10^{-3}$ m
	radius	$30.49 * 10^{-3}$ m
	eccentricity	$4.09 * 10^{-3}$ m
	roughness (RMS)	$0.12 * 10^{-6}$ m
	material	16 Mn Cr 5 E
	hardness	HRC 60
Follower		
	reciprocating mass	2.51 kg
	plate roughness (RMS)	$0.01 * 10^{-6}$ m
	ditto incl. transducers	$0.07 * 10^{-6}$ m
	material	X155CrVMo 12 1
	hardness	HRC 60
Spring stiffness		$5.68 * 10^{4}$ N/m
Filters		
	hydraulic	$3.0 * 10^{-6}$ m
	absolute	$3.0 * 10^{-7}$ m
Oil	SAE classification	85W-140
	viscosity (30 C)	$0.61\ Ns/m^2$
	press.visc.coefficient (30 C)	$2.81 * 10^{-8}\ m^2/N$

Table I. Some numerical data of the cam-follower test rig.

Unless it is stated otherwise, all experiments are carried out at 5.00 s^{-1} shaft speed and 750 N ± 235 N constant load.

Fig.5 shows a detail of the test rig. The camshaft is removed to allow a view on the follower plate with transducers.

4 LUBRICATION MODE

Before any local measurements are carried out, it is necessary to make certain that full film conditions can be attained. Within the regime of full film lubrication a subdivision can be made into parched (38), starved, and fully flooded lubrication. The latter can be subdivided again into 4 subregimes (6), EHD lubrication (designated by VE in Fig.1) being one of them.

4.1 Global film thickness measurements

Full film conditions in the cam-follower contact can easily be checked by a measurement of the Ohmic resistance or the capacitance of the film. For this, the follower plate is insulated by a 5 mm. perspex layer. In addition, the follower is insulated from the test rig mass by the hydrostatic bearing, and at the load cell and the guide blocks of the follower body.

First, the electrical insulation at the

camshaft ball bearings was checked by measuring the capacity over these bearings. A custom modified SKF Lubcheck Mk2 was employed. At 750 N (average load) and 2.5 s^{-1} oil film breakdown occurred at the rising flank of the cam. At speeds over 3.00 s^{-1} there was no breakdown.

Next, the resistance of the oil film during a cam cycle was determined, using a voltage divider. This device has several settings and gives a maximum of 20 mV over the contact. Fig.6 gives a result. The noise in Fig.6a emenates from a 50 Hz interference source, which could not be located. It follows from Fig.6 that the film resistance is in betweeen 3.6 kΩ and 10 kΩ. Therefore, full film conditions actually exist during a cam cycle. Actually, an entire seperation of cam and follower already prevails at 3.00 s^{-1} shaft speed, because the resistance is more than 360 Ω.

Eventually, global capacitance measurements were carried out, using the Lubcheck capacitance monitoring system. A typical result is presented in Fig.7. The film thickness values in this and following Figures is calculated by Dyson et al's (39) method. At maximum follower lift the number of cycles (time base) starts, so θ=0.

4.2 Surface layer formation and running-in

Full film theory does not take account for the formation of thick surface layers. At high sliding speeds a chemical film may form (40), which will set an upper limit to the speed.

Indeed a sudden rise in the global film thickness could be detected. If a worn sliding area of the follower plate is used, resulting in a low Λ value (relative film thickness), surface films will form even at 5 s^{-1} shaft speed within 1800 s. When a fresh part of the plate surface is used, reaction films can develop at speeds over 13 s^{-1} after 2500 till 5000 s. See Fig.8b. In this Figure surface layers are formed after about 700 s, probably initiated by a short period of slightly increased speed. If these layers are formed on the follower surface, an even number of capacitance jumps is needed, see Section 3. In addition, when employing an eccentric cam, they have to be located symmetrically around θ= 0. This is not the case. Consequently, the surface layers are on the cam and not on the follower. A possible explanation is the high content of Cr in the follower plate material (41).

The development of a surface layer is a dynamic phenomenon, in that the layer can change in position and extent in time, see Fig. 8c. Several times a reaction film was initially formed on the end of the rising flank, next grew in extent (not in thickness), and moved slowly to the beginning of the returning flank. This is indissolubly related to changes in the surface roughness during running in. In most cases the reaction layer was removed after coasting down to a lower speed (Fig.8d) or coming to a complete stop.

If it is assumed that the reaction layer has the same dielectric constant as the oil, the layer thickness can be estimated. In Fig.8b and c the reaction film has a thickness of the order of 0.4 μm, which is the same as found by Georges et al (40), and Johnston et al (41). Georges et al (40) use surface profile and resistance readings to detect chemical films formed under pure sliding and high speed, while Johnston et al (41) employ optical interferometric and resistance measurements to investigate films developed under high sliding. The capacitance method can give quantitative information on film thickness, while the resistance method is only qualitatively. In addition, it can be used in engineering situations (lubricated steel-steel contacts), which gives it an advantage over interferometric methods.

Chemical films can only develop at elevated temperatures, typically over 80 C. Therefore, the temperature should be kept low.

If a new sliding area is used, film breakdown does not occur. A sliding area which has been used before should be avoided. In that case, cam and follower have to run-in again with a high initial roughness, leading to high local temperatures and hence surface layer development. It is shown up here that anti-wear additives are effective in cam mechanisms. In this respect, this work is an extension of Johnston et al.'s (41) investigations to more hostile conditions.

After running-in no film breakdown could be detected. If the load is increased to 1250 ± 250 N, and the speed decreased to the minimum speed of 2.45 s^{-1}, there are still no asperities in contact. Coasting down from these adverse conditions results in Fig.9.

4.3 Quasi-stationary lubrication in harmonic cams

Very often entrainment velocities are high and contact lengths are short, resulting in a very short passage time of the fluid in the contact. A lubricant molecule will hardly 'feel' any variations during its passage through the contact. Gu (42) presents a qualitative criterion for the applicability of quasi-stationary analyses at lubrication problems. A contact can be considered stationary, if the passage time is much smaller than the contact duration time. But his concept of contact duration time is not well defined, and in the case of cam mechanisms it could be infinity. Nevertheless, it can be concluded that many concentrated contacts which seem to be dynamically loaded at first sight, show a quasi-steady behaviour. An eccentric cam, having an eccentricity much smaller than the radius, could be one of them.

An initial study into the behaviour of dynamically loaded concentrated contacts has been completed recently and will be published later (43). It is an improvement of Vichard's analysis (10). The computer programme of (43) was used to obtain film thickness versus time plots for an eccentric cam-flat follower contact, for two sets of operating conditions. Figs.10 and 11 show results for 750 ± 250 N, and 1250 ± 250 N, respectively. The dimensionless film thickness behaviour can be described by two dimensionless numbers, viz.

squeeze number:

$$g_s = \frac{1}{2\pi R_r} \left\{ \frac{8\, F^* R_r}{\pi\, l\, E_r} \right\}^{1/2} = \frac{w\, b^*}{2\, u^*}$$

entrainment number:

$$g_w = \frac{1}{2\alpha\eta_o u^*} \left\{ \frac{2\, F^{*3}}{9\pi^3 l^3 E_r^3 R_r} \right\}^{1/2}$$

The squeeze number can be considered as a quantifiquation of Gu's (42) criterion. The reference film thickness h^* is the steady state film thickness under reference speed and reference load conditions. Figs. 10 a and 11 a show the quasi-stationary film thickness h_{quast} / h^*, Figs. 10 b and 11 b present the dynamic behaviour of the minimum film thickness h_{min} / h^*, and Figs. 10 c and 11 c the deviations in minimum film thickness from the quasi-steady solution, all as a function of time θ. Fig. 10 b and 10 c show that this problem is an initial value problem. From these plots it can be concluded that deviations are within 0.3 %. Therefore, an eccentric cam profile, which is only an introduction to more complex shapes, can be considered as quasi-stationary. Note that the squeeze effect increases the load capacity under normal approach ($0.5<\theta<1.0$), but acts in an opposite way under detaching conditions ($0<\theta<0.5$).

If the conditions in a lubricated concentrated line contact may be treated as steady state, the film thickness can also be found from dimensionless charts as provided by Moes (44) or Johnson (45). The representation by Moes lends itself pre-eminently to curve-fitting purposes, while Johnsons map is more appropriate to ascertain the physical effects playing a role. In Fig. 12 the cam cycle is marked in the Johnson map. The medium load cycle is depicted by 1-1, the high load cycle by 2-2. Symmetric cams will always be represented by lines rather than loops. The crosshatched parallelogram is the area investigated by Dowson and Higginson (4). The denser shaded part represents the intermediate EHD lubrication region. It follows from this Figure that the medium load case (750 ± 250 N) is in the intermediate region, whereas the high load case (750 ± 250 N) is just in the EHD region. The numbers in Fig. 12 are defined by Johnson as

$$\text{elasticity number: } g_E = \left\{ \frac{F^2}{\eta_o u E_r l^2 R_r} \right\}^{1/2}$$

$$\text{viscosity number } g_v = \left\{ \frac{\alpha^2 F^3}{\eta_o u R_r^2 l^3} \right\}^{1/2}$$

$$\text{film thickness } \bar{h} = \frac{h_{min} F}{\eta_o u R_r l}$$

The representation in both maps (44,45) has the drawback that varying load and/or speed will affect all three dimensionless groups, including the film thickness. For that reason Fig.1 was drawn, which is purely another representation of the same data. The numbers in Fig.1 are already indicated by Johnson (45):

$$\text{load number } g_F = \left\{ \frac{\alpha^2 E_r F}{R_r l} \right\}^{-1/2}$$

$$\text{speed number } g_u = \left\{ \frac{\alpha^4 E_r^3 \eta_o u}{R_r} \right\}^{1/4}$$

$$\text{film thickness } H = (\alpha E_r)^2 \frac{h_{min}}{R_r}$$

Fig. 13 shows the two cam cycles indicated by 1-1 (medium load), and 2-2 (high load), respectively. The Dowson and Higginson region is again crosshatched.

There is another advantage in this representation. If the composite surface roughness is known, relative film thickness values for Λ can be represented by lines. And so it is possible to indicate critical Λ values. In Fig.13 Λ_{ecc} indicates $\Lambda=1$ for the eccentric cam. As the cam cycles are located at Λ-values an order of magnitude higher, it must be possible to have full film lubrication. The experiments described in Section 4.1 confirm this.

5 INSTRUMENTATION

A brief historic review of the development in vapour deposited transducers for lubricated concentrated contacts can be found in (32). Since then Frey (33) and Baumann (46) completed their experiments with a cam-flat follower and a 2 disc machine. They measured pressure and temperature distributions using thin film microtransducers.

There are only a couple of papers on local film thickness measurements by means of these microtransducers, and they all concern 2 disc experiments. Experiments with dynamically loaded contacts seem to be welcome.

5-1 Thin film microtransducers

The microtransducers used in highly loaded lubricated contacts must meet some stringent requirements. These include:

- high resolution
- fast transient response, RC-time
- small interference with substrate surface topography
- small perturbation of stress and temperature patterns on the substrate surface
- high sensitivity to changes in parameters to be measured
- applicability on heat treatable steels
- good adhesion to the substrate
- low wear (sufficiently long life)

Generally, vapour deposited transducers can meet these requirements. Almost all investigators in this field favour SiO_x as an insulating layer. But the electrical, mechanical and thermal properties differ substantially from steel, thus affecting the temperature in the contact. A material with more steel-like properties is Al_2O_3, and should therefore be preferred. Titanium is used for temperature transducers, because it has a very low pressure sensitivity. As capacitance transducers require only that the material be a good conductor, the same materials can be used as for the temperature transducer. The only difference is in the geometry used.

The electrical resistance R can be made in any arbitrary value. Owing to the processing equipment a value of about 1 kΩ was chosen. The conductor pattern should have a much lower resistance, and is therefore made of gold. To keep the parasitic capacitance C_{par} low, and to avoid pinholes, the conductor pattern area is kept small. The terminals of the conductor pattern are connected to a print board by 20 µm dia. gold wires. Fig. 14 gives a schematic drawing of a thin film transducer.

The transducers can be made by (a) vapour deposition through a mechanical mask, or (b) by vapour deposition followed by laser beam cutting (16) or by a photolithographic process.

In this case photolithography was adopted. It is a very versatile technique. All layers are deposited in one sequence, without breaking the vacuum of the evaporation jar. The layers are partially removed by a selective etching technique, using a photomask. What remains are the conductor and transducer patterns. If desired, a protective coating can be deposited on top of these layers after etching.

Photolithography enables complicated transducer shapes and the manufacture of many transducers together on the same substrate. Flexible photomasks will easily accomodate to the substrate curvature.

Fig.15 shows an example of the geometry of the transducers used in the experiments of section 6. The temperature transducer (top two in Fig.15), can be positioned at any wanted location. The upper capacitance transducer (bottom two in Fig.15) necessitates a rotating contact from the camshaft to the fixed world. The lower capacitance transducer gets around this problem, but has a lower resolution.

5.2 Signal processing

In most cases a Wheatstone bridge, or a compensation circuit is used when small changes in Ohmic resistance are to be measured. In this case a new design was used, in which a reference resistance is not needed (Fig.16). A constant electric current of 1 mA flows through the transducer, which corresponds to a certain voltage drop. The difference with an externally adjustable reference voltage is amplified by a broadband instrumentation amplifier (50 x). High quality, low noise operational amplifiers are used, resulting in a large bandwidth and a high slew rate. To obtain maximum sensitivity of the dynamic signal, the reference voltage can be adjusted for small changes in resistance due to operating temperature variations. The absolute temperature can now be deduced from the reference voltage.

The capacitance is measured by an SKF Lubcheck Mk II capacitance monitoring system (47).

The high frequency output signal is sampled by a digital transient recorder. In most experiments a sample rate of 0.2 ms. was used. In film thickness geometry studies a sample rate of less than 10 μs is needed (at 5 s^{-1} shaft speed).

6 MEASUREMENTS

In earlier experiments (32) it was found that under the same operating conditions large differences in the local temperature can occur. At the same spot and point of time the temperature increase could well be 1.5 C, but also 15 C. A slight misalignment in the cam-follower contact was thought to cause different lubricant conditions across the contact. The transducer layout (Fig.15) permits temperature measurements at different axial positions, allowing capacitance measurements at the left and right side of the contact. Thus it is possible to investigate the assumption that the contact may be considered as a line contact.

6-1 Capacitance measurement under misalignment

Fig.17 offers a first impression of the film thickness formation. The capacitance transducers used in this experiment are both positioned 3 mm under the center line, one at the left, the other at the right side. The most salient feature is the difference between the left and right capacity variations. The largest minima occur shortly after maximum lift, where about 0.2 μm (at the left) and 0.85 μm (at the right) minimum film thickness occurs, indicating a misalignment of about $5 * 10^{-5}$ rad. The other extrema are approximately 0.4 μm, and 2.2 μm, respectively, suggesting a misalignment of about 10^{-4} rad. Hence in spite of all precautions, there are no line contact conditions.

Obviously, the left side of the contact is more heavily loaden. This was also justified by wear scars at the same side.

There are many experiments supporting the diagnosis of misalignment. Fig.18 is the result of another experiment, where a new follower plate has been used. Here the left side transducer indicates a minimum film thickness of about 0.4 μm at maximum follower lift. What happens when the load is increased, can be seen in Fig.19. The minimum film thickness drops to a value of about 0.3 μm at 1500 N.

A perfect line contact is difficult to realize, but it should be pursued. Therefore a self-aligning elastic hinge support was designed, which is located between follower body and plate, see Fig.20. All results from the next section are obtained using this device.

6-2 Capacitance and temperature measurements

Due to time constraints it was not possible to carry out film thickness measurements as in Fig.17, that is with two transducers located along the same line. Instead of this, two opposing temperature transducers (see Fig.15) were positioned at 4.20 mm and 5.20 mm under the center line, resulting in Fig.21A and B. The minimum film thickness at the right is about 0.7 μm, at the left 0.8 μm for the first extrema, and about 0.9 μm (right) and 0.8 μm (left) for the second extrema in Fig. 21 A, and 1.1 μm (right) and 1.0 μm (left) in Fig.21 B. Obviously, the second conductor wire is located at the point of maximum contact sweep on the follower plate. The conclusion is near that the alignment in the contact is much better now at $5\ 10^{-6}$ rad. This should be supported by temperature measurements.

Fig.22 was obtained under exactly the same conditions as Fig.18, except that the elastic hinge support is mounted between follower plate and follower body. The minimum film thickness is about 0.5 μm.

Eventually Fig.23 was obtained. This Figure demonstrates the possibility to scan the complete cam cycle using only one transducer.

Figures 24, 25, and 26 show some comparisons between left and right side temperatures on the follower plate. In Fig.24 and 25 the long transducer type was used, in Fig.26 the short type (Fig.15). The cam cycle temperature is scanned in Fig.27.

7 DISCUSSION

From Fig.17 it can be concluded that misalignment of the order of 10^{-4} rad occurs.

This may not seem large, but it should be viewed on the very thin film thickness scale. The Figures presented in this paper could lead to the conclusion that the left side of the follower plate is always on the heavy load side. Many other experiments falsify this. The misalignment problem can only be alleviated by a self aligning support.

Another feature of the local capacitance measurements from Fig.17 are the parasitic capacitances between transducer and substrate, and between substrate and cam. This results in a low shaft speed frequency capacitance variation, as obtained in global capacitance measurements, see Fig.7. These parasitic capacitances can be made smaller by employing a thicker insulating layer.

Under increased loads the film thickness profile develops a constriction at the heavy load side, as can be found in Fig.19. This film thickness dip is well known in steady state EHD lubrication. It is important, because the film thickness minimum will often be found here. This reduction in film thickness would not have occurred if the cam-follower contact were perfectly aligned.

Without the elastic follower plate support, maximum temperature variations were found to be 16.4 C at maximum lift on the left (heavy load) side, measured with a long type transducer. A short type, having its sensor more outwards, would definitely have detected a higher temperature.

After mounting the elastic support, alignment was improved by an order of magnitude. Temperature differences in axial direction are low. It should be kept in mind that Figs.24 and 25 were obtained with a long type transducer, and Figs.26 and 27 with a short one. The distance between two opposing transducers is about 6.25 mm for the long type, and 11.25 mm for the short type. Hence the maximum temperature change of 14.5 C is probably much lower than the corresponding value without a self-aligning device. Note that in Fig.27 the temperature increase is maximum at about 1.80 mm before maximum lift.

Under isothermal conditions the minimum film thickness can be estimated by employing empirical formulae, like the Dowson and Higginson expression (4). At 40 C follower plate temperature it can be found that the steady state minimum film thickness amounts about 1.8 μm at maximum lift, and about 1.6 μm at minimum lift. This is in contrast with the experimental findings. The measurements show that (1) the film thickness is much smaller, and (2) the film thickness at maximum lift is always smaller than the film thickness at minimum lift. It is known from steady state EHD lubrication that the oil inlet temperature plays a decisive role in film thickness calculations. First, the inlet position needs to be known as a function of time, and next temperature measurements must be carried out at that location. From Fig.27 it can be concluded that the contact temperature at maximum lift rises about 12 C, and at minimum lift about 1C. At 55 C and maximum lift the steady state minimum film thickness will drop to 0.8 μm. Hence temperature effects cannot remain out of it, but also they cannot explain the difference comprehensively. A 60 C temperature rise at maximum lift is needed to obtain film thicknesses as low as 0.2 μm, which can develop under misalignment conditions. At these temperatures reaction layers formation can be expected (41). However, the temperature increase at minimum lift is far too low to explain the measured values. It could be that starvation occurs. This will be investigated later by local pressure measurements.

Capacitance field deviations and conductor pattern effects may result in capacitance reading errors. The photolithographic technique allows for complicated transducer shapes. Therefore these problems can be tackled by employing guard shields and conductor patterns, permitting 3-point or 4-point measurements.

So far, transducer signals are stored and reproduced directly. Signals are acquired at a certain spot as a function of time. They need processsing to be able to compare them with numerical simulations, i.e. a representation at a certain point in time as function of position. This automatization will be realized in the near future.

An eccentric cam is not the best example of a real dynamically loaded concentrated contact. This study is rather an introduction to the experimental techniques for this type of contact, than an exhaustive experimental investigation. Many automotive cams have a momentarily zero entrainment effect. This will be the subject of a forthcoming paper.

Most follower plates did show some wear after some time. Occasionally no wear was observed, after 15 hrs. of running, which is sufficient for laboratory applications.

8 CONCLUSIONS

Vapour deposited transducers were used in an eccentric cam-flat follower contact. Temperature and film thickness measurements were carried out as an introduction to experiments in dynamically loaded concentrated contacts.

If the contact has some misalignment, mixed film conditions may prevail at the heavy load side. The rise in film temperature can become high, leading to chemical reaction layer formation. The capacitance measuring technique allows an examination of the extent and thickness of these layers.

Good alignment was obtained after incorporating a self-aligning elastic hinge support. The measured temperature variations are not high, but need to be included in film thickness calculations. Probably starvation occurs, because calculated film thicknesses are still too high. The transducers worked well and have a satisfactory life expectancy. Further experimental studies, incorporating film thickness, temperature, and pressure measurements in a cam-follower contact having momentarily zero entrainment action, are needed.

9 ACKNOWLEDGEMENTS

The authors gratefully acknowledge the contribution of L.Kodde, for his advice on instrumentation, and R.A.F.König, for his help in the manufacture of the transducers. This

work was partly carried out under a contract of the Dutch Foundation for Applied Sciences STW which is appreciated very much.

References

(1) MARTIN,H.M. "Lubrication of gear teeth", Engineering (London), 1916, 102, pp. 119-121 and p.527.

(2) GRUBIN,A.N. "Fundamentals of the hydrodynamic theory of lubrication of heavily loaded cylindrical surfaces", in: Investigation of the Contact of Machine Components", by Kh.F.Ketova (ed.), Central Scientific Research Institute for Technology and Mechanical Engineering (TsNITMASh), Book No. 30, Moscow 1949 (D.S.I.R. Translation No. 337), pp. 115-166. Note: this reference is almost identical to ref.(7).

(3) BLOK,H. Discussion. Gear Lubrication Symposium, Part I, The Lubrication of Gears, Journal of the Institute of Petroleum, 1952, 38, pp.673-683

(4) DOWSON,D., and HIGGINSON,G.R. Elastohydrodynamic Lubrication, SI (2nd) edition, 1977 (Pergamon, Oxford)

(5) HERREBRUGH,K. "Solving the Incompressible and Isothermal Problem in Elastohydrodynamic Lubrication Through an Integral Equation", Journal of Lubrication Technology, ASME Trans.1968, 90, pp.262-270

(6) HAMROCK,B.J., and DOWSON,D. Ball Bearing Lubrication, 1981 (Wiley New York)

(7) ERTEL,A.M. "The Calculation of Hydrodynamic Lubrication of Curved Surfaces under High Loads and Sliding Motion "'(in German) Fortschritt-Berichte der VDI-Zeitschriften, Vol.1, No.115, edited by O.R.Lang and P.Oster,1984, 92 pp. Note: This work is believed to be Ertel's Ph.D.Thesis, TsNITMASh, 1945, published by his advisor Grubin (2).

(8) CHRISTENSEN,H. "The oil film in a closing gap", Proc.Roy.Soc.Lond., Series A, 1962, 266, pp.312-328

(9) HERREBRUGH,K. "Elastohydrodynamic Squeeze Films Between Two Cylinders in Normal Approach", Journal of Lubrication Technology, ASME Trans. 1970, 92, pp. 292-302.

(10) VICHARD,J.P. "Transient effects in the lubrication of Hertzian contacts", J. Mech. Engng. Sci., 1971, 13, pp. 173-189

(11) HOLLAND,J. "Instationary EHD Lubricants", (in German), Konstruktion, 1978, 30, pp. 363-369

(12) HAIQING,Y.,XIAZE,Z., and YUXIAN,H. "The computation of unsteadily loaded EHL film thickness and other lubrication parameters of cam-tappet pairs of IC engines and analysis of their performance", in: Developments in Numerical and Experimental Methods Applied to Tribology, Paper VII(iii), Butterworths,London, 1984, pp.171-181

(13) OH,K.P. "The Numerical Solution of Dynamically Loaded Elastohydrodynamic Contacts as a Nonlinear Complementarity Problem", Journal of Tribology, Trans. ASME, 1984, 106, pp. 88-95

(14) PAUL,G.R., and CAMERON,A. "An absolute high-pressure microviscometer based on refractive index", Proc.R.Soc.Lond.A., 1972, 331, pp.171-184

(15) PAUL,G.R.,and CAMERON,A. "The ultimate shear stress of fluids at high pressures measured by a modified impact microviscometer", Proc.R.Soc.Lond.A., 1979, 365, pp. 31-41

(16) SAFA,M.M.A., and GOHAR,R. "Pressure Distribution Under a Ball Impacting a Thin Lubricant Layer", Journal of Tribology, Trans.ASME, Series F, 1986, 108, pp. 372-376

(17) HAMILTON,G.M., and MOORE,S.L. "The lubrication of piston rings. First paper: measurements of the oil-film thickness between the piston rings and liner of a small diesel engine", Proc.Instn.Mech.Engrs., 1974, 188, pp.253-261

(18) MOORE,S.L.,and HAMILTON,G.M. "Ring pack film thickness during running in", in: The Running-in Process in Tribology, Paper VII(ii), Butterworths, Guildford, U.K., 1982, pp. 153-161

(19) PARKER,D.A., STAFFORD,J.V., KENDRICK,M., and GRAHAM,N.A. "Experimental measurements of the quantities necessary to predict piston ring-cylinder bore oil film thickness, and of the oil film thickness itself, in two particular engines", in: Piston Ring Scuffing, Mechanical Engineering Publications, London, 1976, pp. 79-98

(20) CLOVER,M.F., and LYNN,F.A. "Factors affecting piston ring scuffing during running-in", in: Piston Ring Scuffing, Mechanical Engineering Publications, London, 1976, pp. 45-59

(21) FURUHAMA,S., ASAHI,C., and HIRUMA,M. "Measurement of Piston Ring Oil Film Thickness in an Operating Engine", ASLE Trans.,1983, 26, pp. 325-332

(22) DOW,T.A., SCHIELE,C.A., and STOCKWELL,R.D. "Techniques for Experimental Evaluation of Piston Ring-Cylinder Film Thickness", Journal of Lubrication Technology, Trans.ASME, 1983, 105, pp.353-360

(23) TODSEN,U. "Investigation of the tribological system piston-piston ring-cylinder liner", (in German), VDI-Forschungsheft, No.628, 1985

(24) DOWSON,D., RUDDY,B.L., and ECONOMOU,P.N. "The elastohydrodynamic lubrication of piston rings", Proc. R. Soc. Lond., Series A, 1983, 386, pp. 409-430

(25) VICHARD,J.P., and GODET,M.R. "Simultaneous measurement of load, friction, and film thickness in a cam-and-tappet system", in: Experimental Methods in Tribology, Proc.Instn.Mech.Engrs., 1967-68, 182, pp.109-113

(26) NINOMIYA,K., KAWAMURA,M., and FUJITA,K. "Electrical Observation of Lubricant Film Between a Cam and a Lifter of an OHV Engine", SAE Paper No.780930

(27) SCHOUTEN,M.J.W. "Elastohydrodynamic Lubrication, Interim Report" (in German), FKM-Forschungsheft No.40,1976

(28) SCHOUTEN,M.J.W. "Elastohydrodynamic Lubrication, Final Report", (in German), FKM-Forschungsheft Nr.72, 1978

(29) HAMILTON,G.M. "The hydrodynamics of a cam follower", Tribology International, 1980, 13, pp. 113-119

(30) SPIEGEL,K. "Contribution to EHD Lubrication of Cam-Follower Pairs",(in German), Ph.D.Thesis, Clausthal University of Technology, Germany, June, 1982

(31) SMALLEY,R.J., and GARIGLIO,R. "The

Role of Tappet Surface Morphology and Metallurgy in Cam/Tappet Life", in: Tribology of Reciprocating Engines, Butterworths, Sevenoaks, 1983, pp. 263-272

(32) SCHOUTEN,M.J.W., van LEEUWEN,H.J., and MEIJER,H.A. "The Lubrication of Dynamically Loaded Concentrated Hard Line Contacts: Temperature and Pressure Measurements", AGARD Conference Proceedings, No.394, San Antonio, TX, April 22-26, 1985, AGARD 1986

(33) FREY,D. "Pressure, Temperature and Load Measurements in an Instationary EHD Contact", (in German), Ph.D.Thesis, Karlsruhe University, Germany, 1985

(34) BAIR,S., GRIFFIOEN,J.A., and WINER,W.O. "The Tribological Behaviour of an Automotive Cam and Flat Lifter System", Journal of Tribology, Trans. ASME, 1986, 108, pp. 478-486

(35) STEINFUEHRER,G. "The Oil Film Thickness at Entrainment Velocity Change. A Contribution to the Tribology of Instationary Motions", Ph.D.Thesis, Hannover University, 1978

(36) COY,R.C., and DYSON,A. "A Rig to Simulate the Kinematics of the Contact Between Cam and Finger Follower", Lubrication Engineering, 1983, 39, pp. 143-152

(37) WATKINS,R.C. "A new approach to the deviation of viscosity in lubricated contacts", in: Eurotrib 85, Vol.I, Paper 2.9, Elsevier, Amsterdam, 1985

(38) KINGSBURY, E. "Parched Elastohydrodynamic Lubrication", Journal of Tribology, Trans. ASME, 1985, 107, pp. 229-233

(39) DYSON,A., NAYLOR,H., and WILSON,A.R. "The measurement of oil-film thickness in elastohydrodynamic contacts", Proc.Instn.Mech.Engrs. 1965-1966, 180, pp. 119-134

(40) GEORGES,J.M., TONCK,A., MEILLE,G., and BELIN,M. "Chemical Films and Mixed Lubrication", ASLE Trans., 1983, 26, pp. 293-305

(41) JOHNSTON,G., CANN,P.M., and SPIKES,H.A. "Phosphorus anti-wear additives: thick film formation and its effect on surface distress", in: Global Studies of Mechanisms and Local Analyses of Surface Distress Phenomena, 12 th Leeds-Lyon Symposium (1985)

(42) GU,A. "Elastohydrodynamic Lubrication of Involute Gears", Journal of Engineering for Industry, Trans. ASME, 1973, 95,pp. 1164-1170

(43) LUYTEN,C.T.P.M. "The dynamic behaviour of heavily loaded EHD lubricated line contacts", M.Sc.Thesis, Eindhoven University of Technology, May 1986

(44) MOES,H. Discusion, Proc.Instn.Mech.Engrs., 1965-1966, 180, pp. 244-245

(45) JOHNSON,K.L. "Regimes of elastohydrodynamic lubrication", J.Mech.Engng.Sci., 1970, 12, pp.9-16

(46) BAUMANN,H. "Pressure and temperature measurements by vapour deposited thin layer transducers in an EHD line contact" (in German), Ph.D. Thesis, Karlsruhe University, Germany, 1985

(47) HEEMSKERK,R.S., VERMEIREN,K.N., and DOLFSMA,H. "Measurement of Lubrication Condition in Rolling Element Bearings", Trans. ASLE, 1982, 24, pp. 519-527

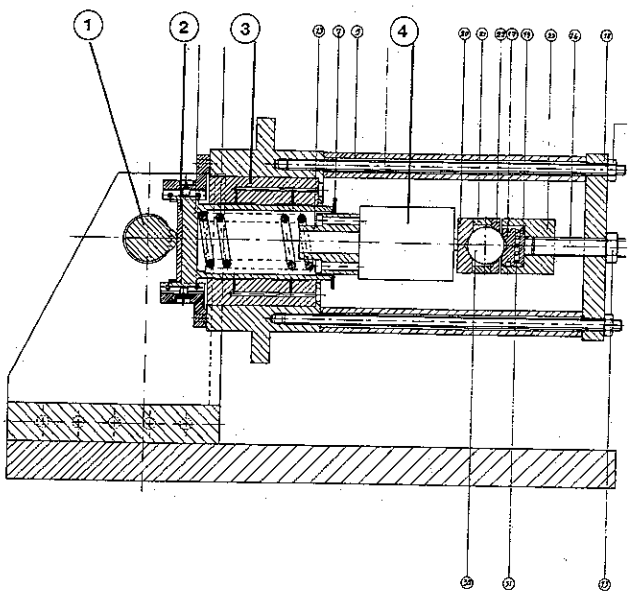

Fig.2 Cam-follower test rig. See text

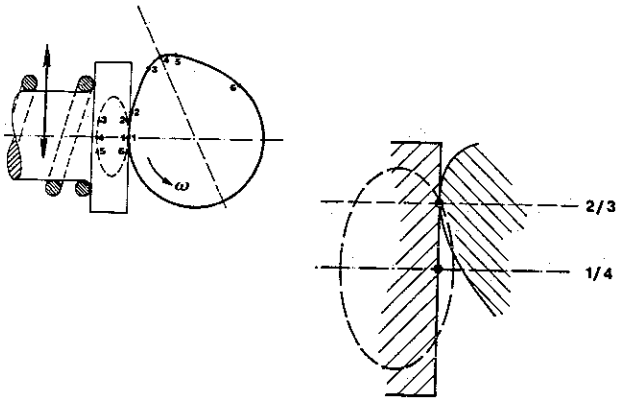

Fig.3 Cam-flat follower measurement principle. See text

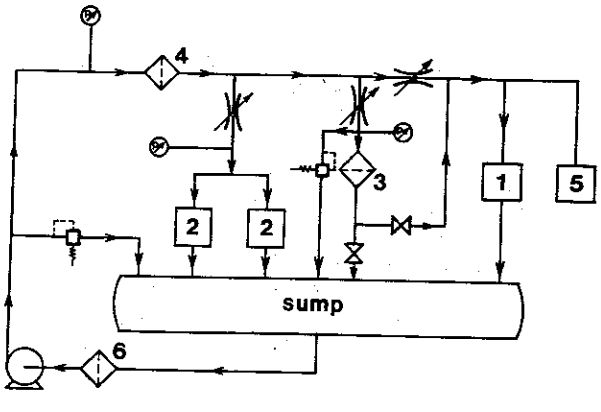

Fig.4 Oil filtering circuit. See text.

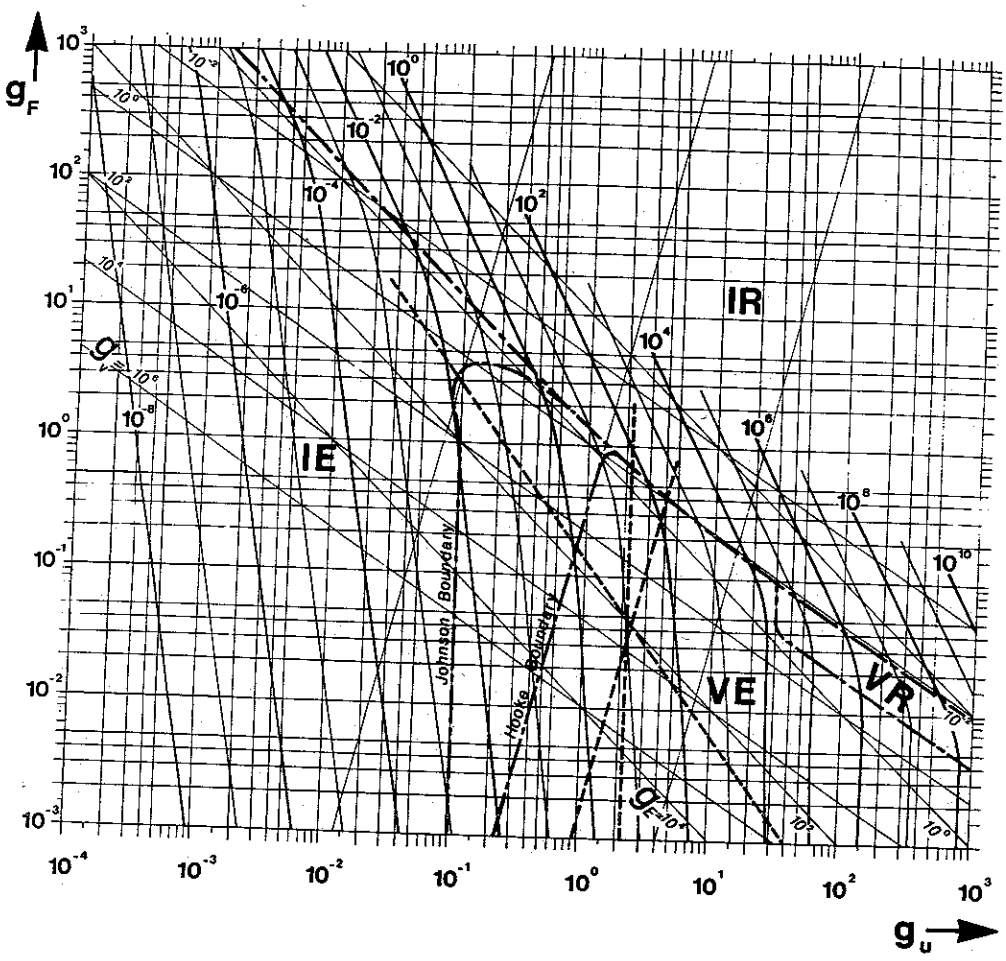

Fig.1. Dimensionless film thickness chart for the steady state case

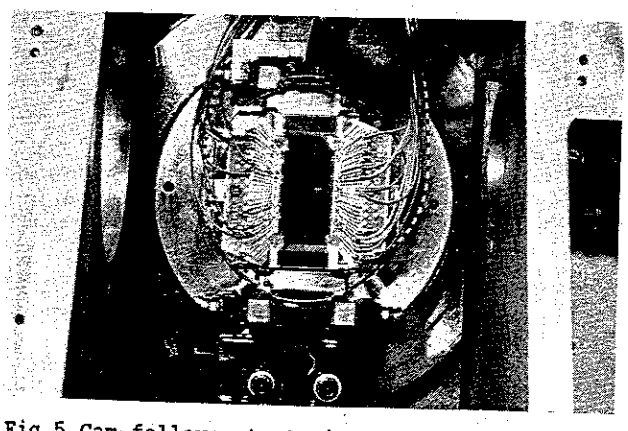

Fig.5 Cam-follower test rig detail; camshaft removed.

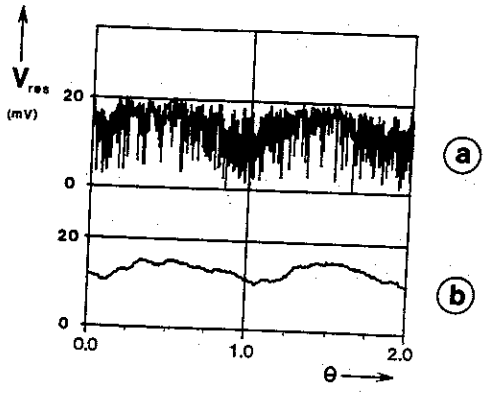

Fig.6 Cam-follower contact resistance, (a) at 3.6 kΩ, 100 kHz LPF; (b) at 3.6 kΩ, 100 Hz LPF

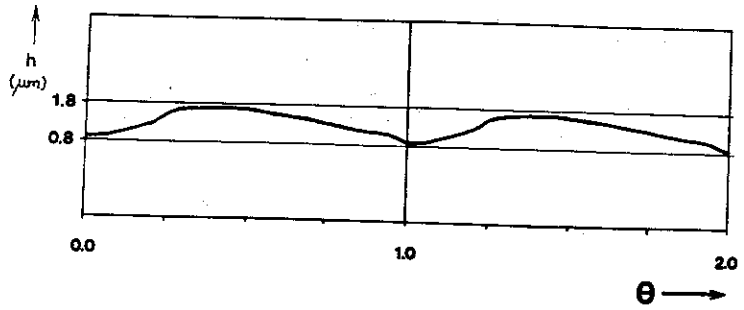

Fig.7 Global capacitance monitor reading at 750 ± 250 N, 5 s^{-1}

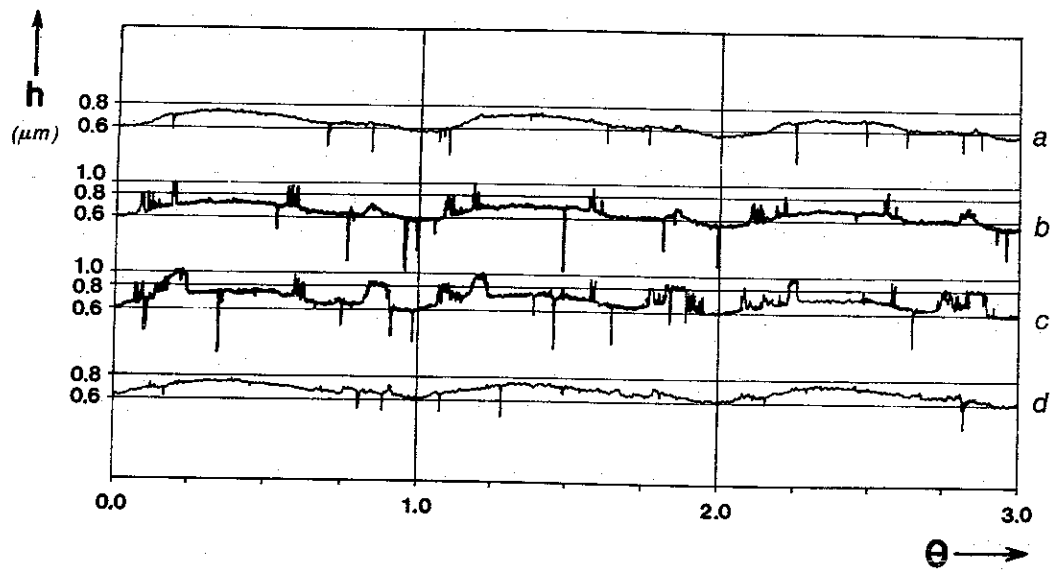

Fig.8 Reaction layer development on the cam surface, (a) at 13.43 s^{-1}, after 600 s; (b) after a short period at 14.00 s^{-1}, after 700 s; (c) at 13.45 s^{-1}, after 1500 s; after 500 s at 5.42 s^{-1}, 2000 s total elapsed time

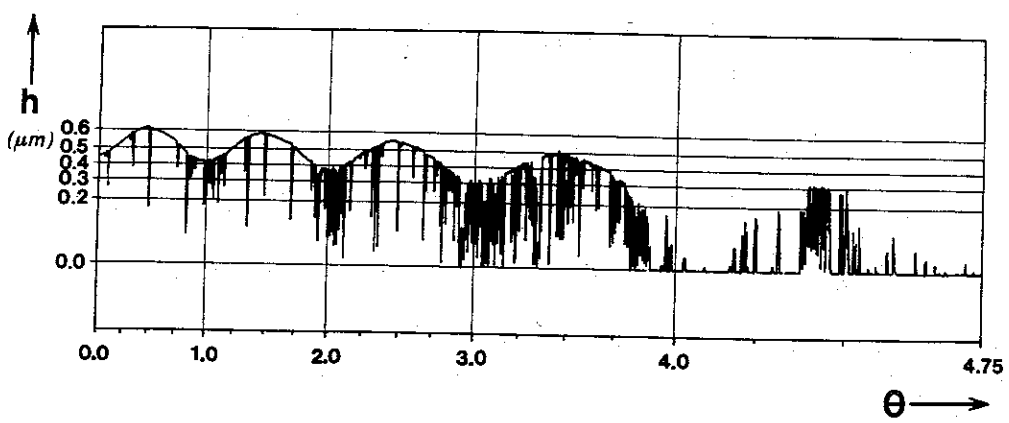

Fig.9 Global capacitance monitor (film thickness) reading under coasting down conditions, initial load 1250 ± 250 N, speed 2.47 s^{-1}

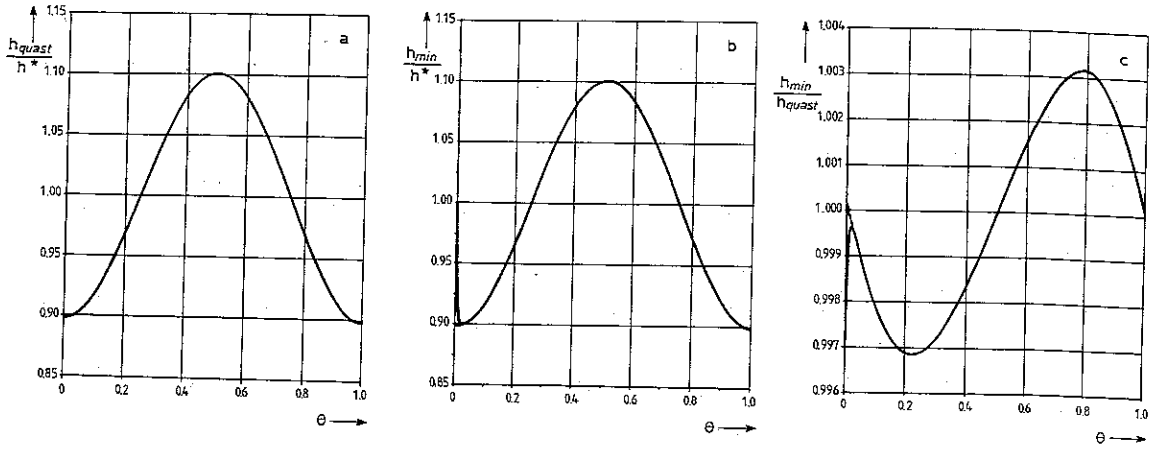

Fig.10 Theoretical film thickness curves for 750 ± 250 N load and 5 s^{-1} shaft speed, g_s=6.28 10^{-4}, g_w=1.58 10^{-3}, (a) quasi-stationary solution, (b) dynamic solution, (c) deviation from steady state

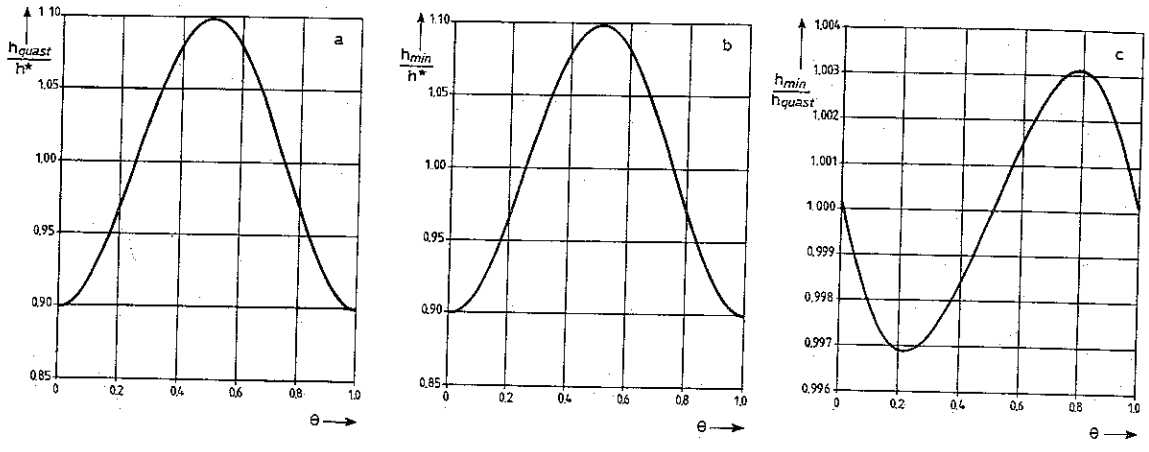

Fig.11 Theoretical film thickness curves for 1250 ± 250 N load and 5 s^{-1} shaft speed, g_s=8.11 10^{-4}, g_w=3.41 10^{-3}, (a) quasi-stationary solution, (b) dynamic solution, (c) deviation from steady state

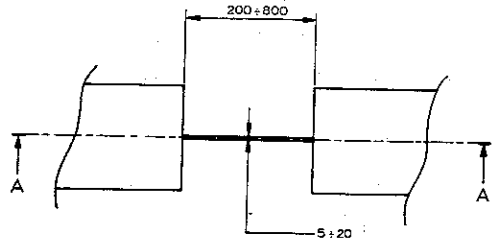

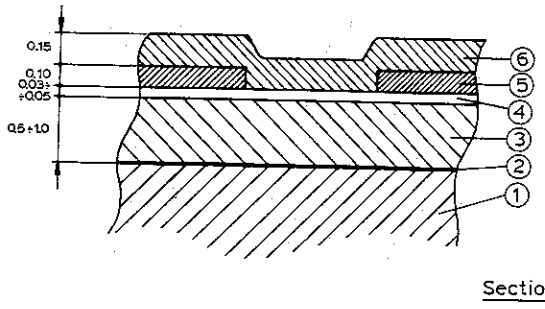

Section A-A

Fig.14 Schematic drawing of a thin film transducer, (1) substrate, (2) adhesive layer, (3) insulating layer, (4) transducer, (5) conductor pattern, (6) protective layer (optional)

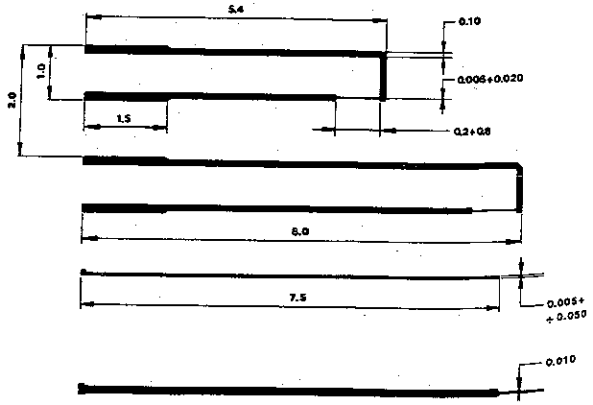

Fig.15 Transducer geometries. Upper two: temperature transducers, lower two: capacitance transducers.

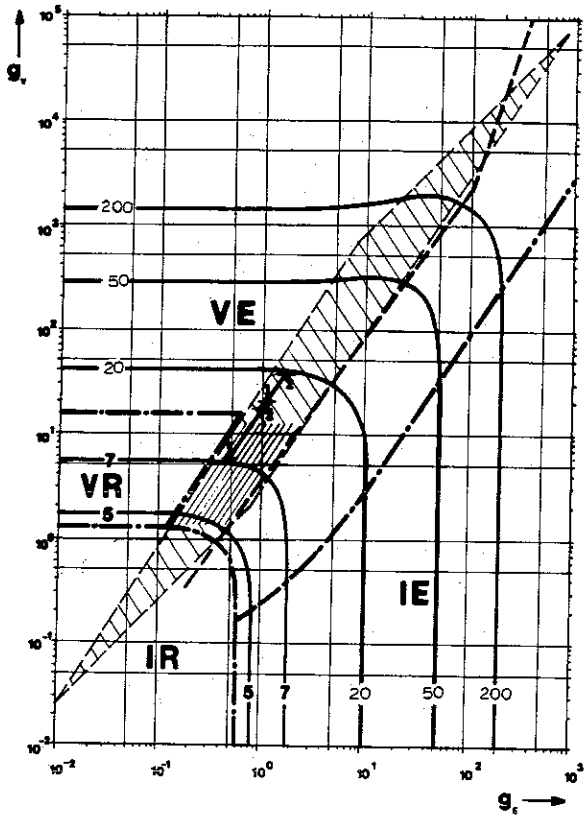

Fig.12 Dimensionless film thickness chart after Johnson (45) showing two cam cycles 1-1 and 2-2

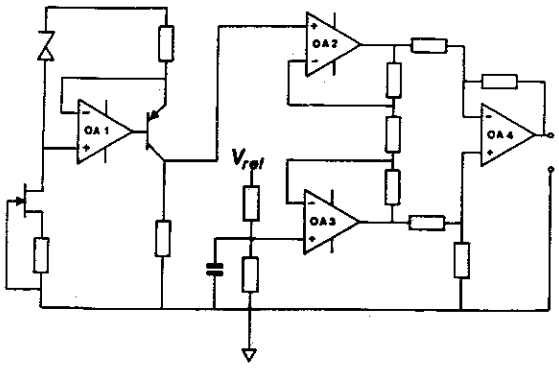

Fig.16 Amplifier (schematic), used in the temperature experiments. R_T: temperature transducer; V_R reference voltage

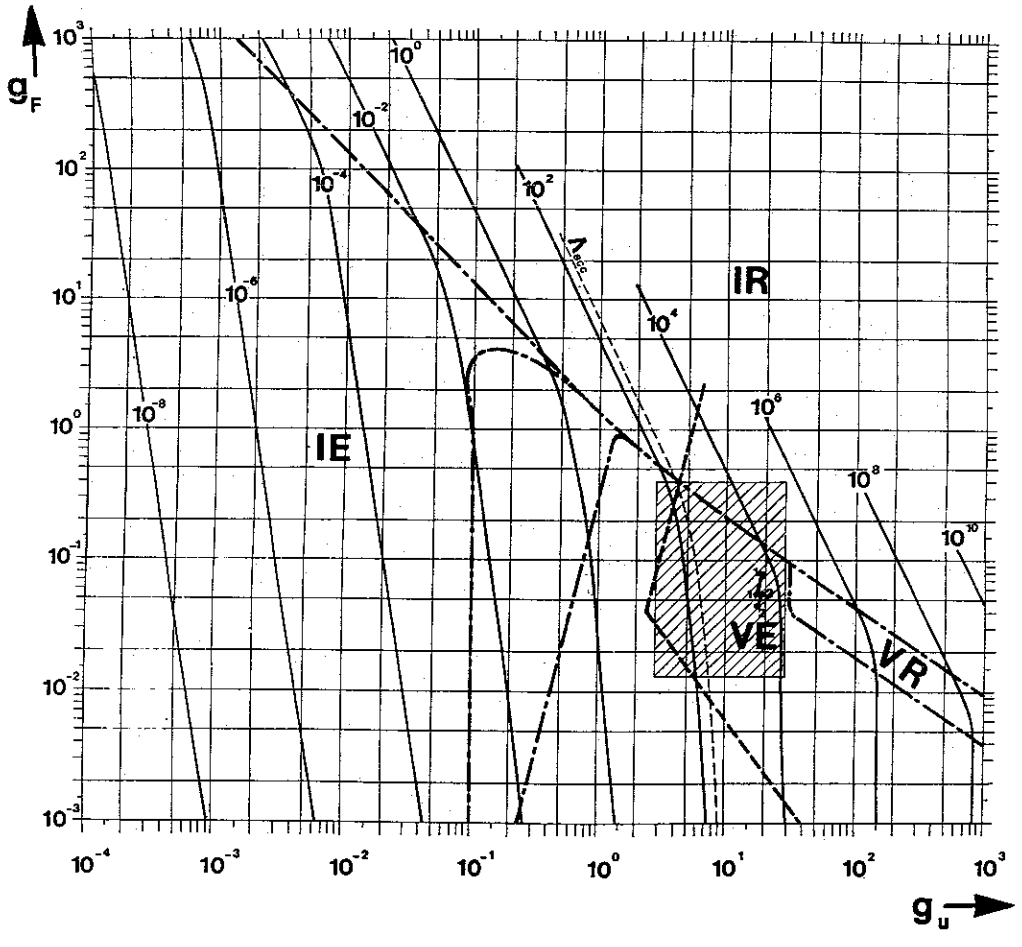

Fig.13 Dimensionless film thickness chart showing cam cycles 1-1, and 2-2

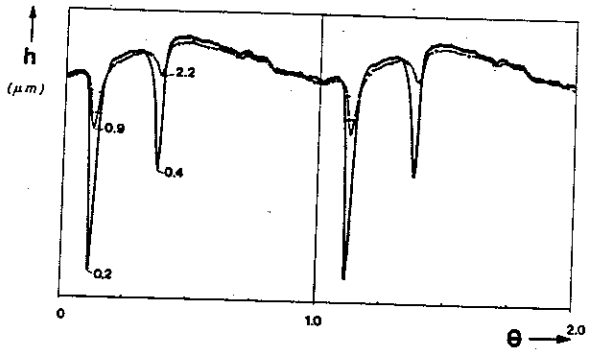

Fig.17 Film thickness at left (___) and right (_._._) side of the cam-follower contact. Transsducer position 3.00 mm under center line.

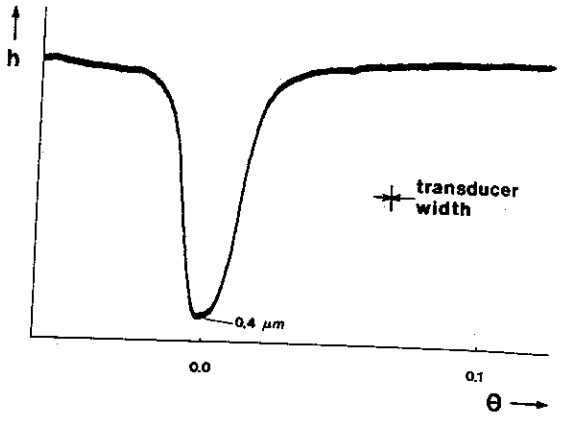

Fig.18 Film thickness at left side of the contact. Transsducer position at center line (maximum lift)

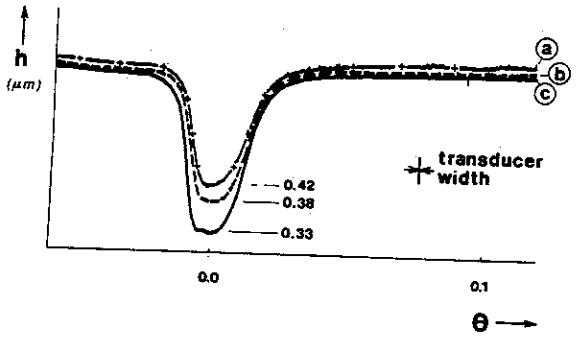

Fig.19 Film thickness at left side of the contact. Transsducer position at center line (maximum lift). (a) 750 ± 250 N, (b) 1000 ± 250 N, (c) 1250 ± 250 N.

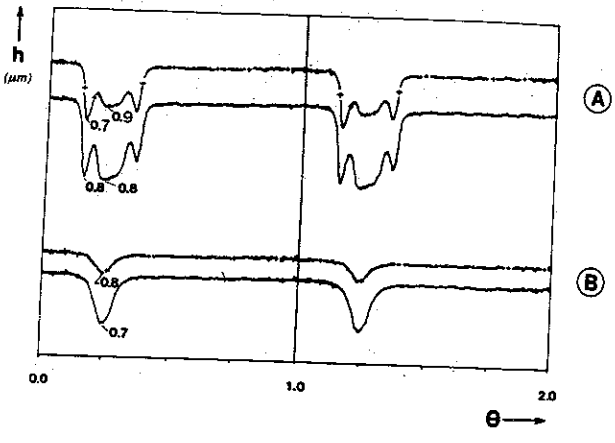

Fig.21 Film thickness at left (____) and right (_._._)side of the contact. Temperature transducer position (a) 4.20 mm, (b) 5.20 mm under center line

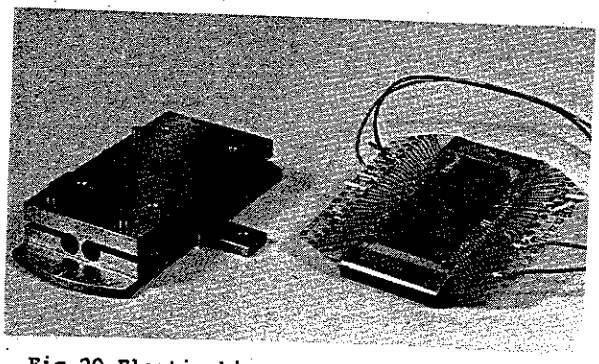

Fig.20 Elastic hinge support and follower plate

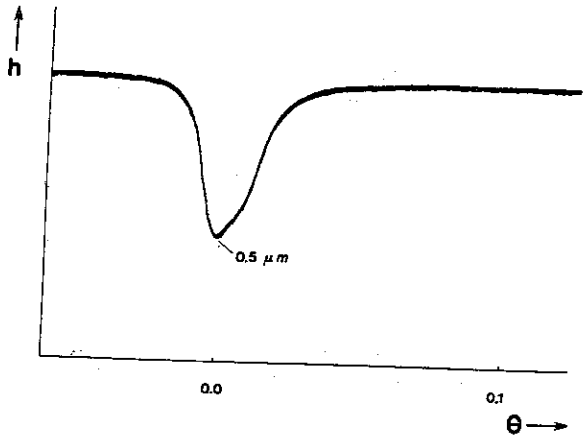

Fig.22 Film thickness at right side of the contact. Transsducer position at center line (maximum lift)

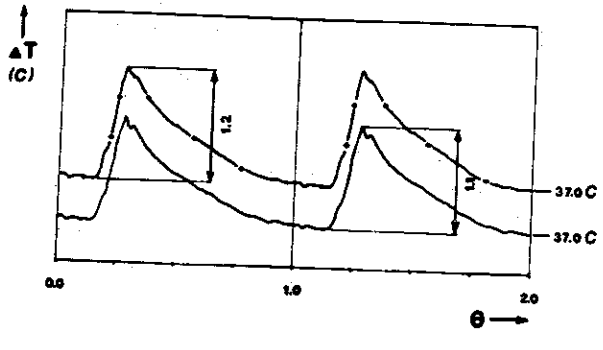

Fig.24 Temperature at left (___) and right (-.-.-) side of the contact. Transsducer position 4.30 mm under center line. Long transsducer geometry.

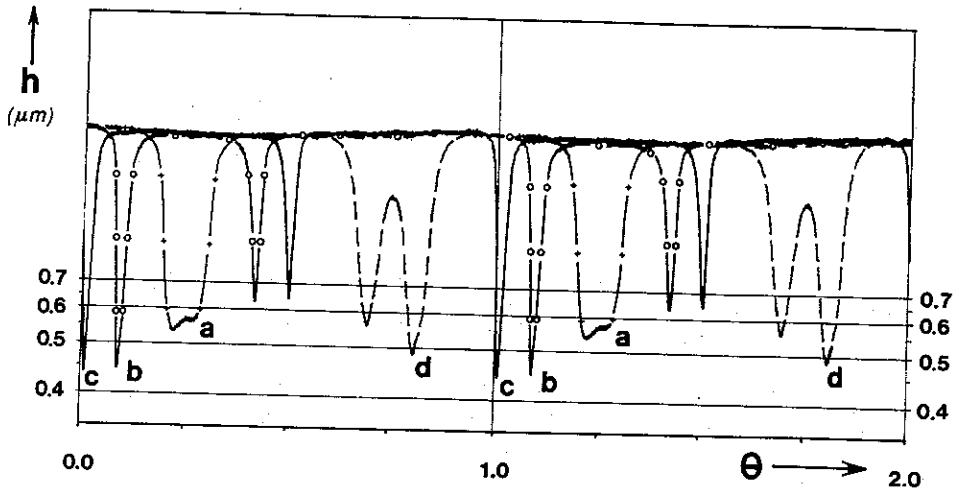

Fig.23 Film thickness at right side of the contact. Transducer positions are (a) 4.05 mm, (b) 2.10 mm, (c) 0.10 mm under, and (d) 3.90 mm over center line

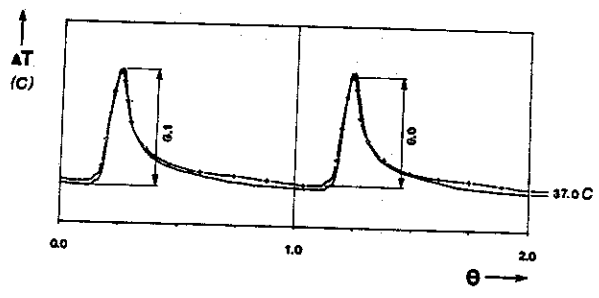

Fig.25 Temperature at left (___) and right (_._._) side of the contact. Transducer position 3.80 mm under center line. Long transducer geometry.

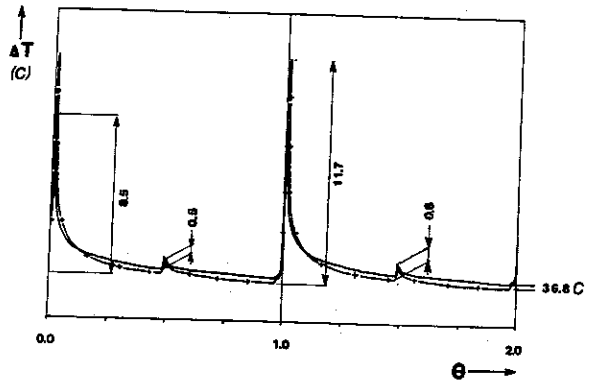

Fig.26 Temperature at left (___) and right (-.-.-) side of the contact. Transducer position 0.20 mm under center line. Short transducer geometry.

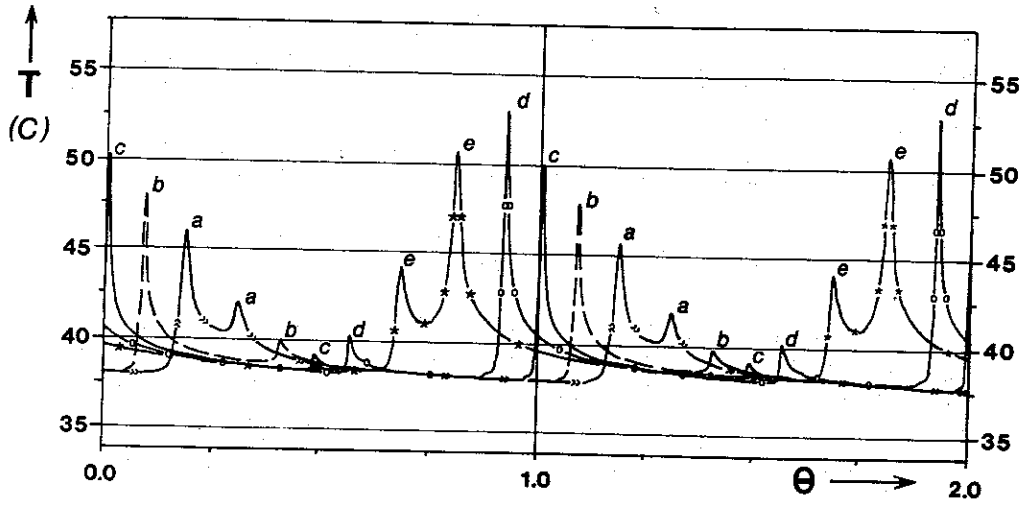

Fig.27 Temperature at right side of the contact. Transducer positions are (a) 3.80 mm, (b) 2.20 mm, (c) 0.20 mm under, and (d) 1.80 mm, (e) 3.80 mm over center line. Long transducer